

# Nucleation of ZnTe on the As-Terminated Si(112) Surface

M. JAIME-VASQUEZ,<sup>1,2</sup> M. MARTINKA,<sup>1</sup> R.N. JACOBS,<sup>1</sup> and  
J.D. BENSON<sup>1</sup>

1.—U.S. Army Research Development and Engineering Command (RDECOM), Communications—Electronics Research, Development and Engineering Center (CERDEC), Night Vision and Electronic Sensors Directorate (NVESD), Fort Belvoir, VA 22060-5806, USA. 2.—e-mail: marvin.jaime@nvl.army.mil

We employ a suite of surface analysis techniques that probe the outermost ZnTe/As-Si(112) surface to generate an understanding of the initial stages of the heteroepitaxial HgCdTe/CdTe/ZnTe/As-Si(112) layer formation. Ion scattering spectroscopy (ISS), reflection-high energy electron diffraction (RHEED), along with nondestructive depth profiles by angle-resolved x-ray photoelectron spectroscopy (XPS) are successfully applied to clarify and support the nucleation stages of ZnTe formation on the As-terminated Si(112) substrate. Data indicate a slow growth of the first ZnTe layer. In addition, no evidence of thick ZnTe island formation exists. The current ZnTe formation process generates full coverage on the Si(112) surface after six to nine MBE cycles. In order to fully understand the details of the ZnTe nucleation process on the Si(112) substrate, we present an inelastic background analysis with the Tougaard method to study surface morphology.

**Key words:** ZnTe/Si (112), ion scattering spectroscopy (ISS), x-ray photoelectron spectroscopy (XPS), nucleation, reflection-high energy electron diffraction (RHEED)

## INTRODUCTION

The Si(112) surface, the current principal substrate for large-area epitaxial growth of HgCdTe thermal imaging and electronic systems, has a substantial lattice mismatch with the molecular beam epitaxy (MBE)-deposited HgCdTe/CdTe epitaxial overlayers. The formation of CdTe on a ZnTe/Si(112) substrate provides a straightforward means of epitaxial deposition of the HgCdTe by MBE. Nevertheless, the unprecedented 19.3% lattice mismatch of Si to HgCdTe is presumed to be the main contributor to relatively high dislocation densities, even for state-of-the-art material. In spite of this, the CdTe/ZnTe buffer layer scheme provides acceptable HgCdTe/CdTe/ZnTe/Si structure quality and electrical characteristics for short wavelength infrared and middle wavelength infrared focal plane arrays (FPAs). Further reduction in dislocation density by at least an order of magnitude is needed for adequate long wavelength infrared HgCdTe FPAs.

The primary role of the initial ZnTe layer is to provide improved B-face nucleation and increased crystallinity for the epitaxial CdTe layer.<sup>1,2</sup> ZnTe exhibits a 12% lattice mismatch with Si, compared to 19.3% for CdTe on Si, resulting in a stepping layer for the subsequent growth of CdTe.<sup>1-7</sup> The method includes the formation of a thin buffer layer of ZnTe on the As-exposed Si(112) surface, followed by the formation of CdTe and subsequent HgCdTe structure. This procedure is used to filter threading dislocations from the underlying ZnTe/Si interface.<sup>6,7</sup> The ZnTe layer is grown using migration enhanced epitaxy (MEE). The MEE promotes a two-dimensional growth mode, while minimizing the generation of growth defects.<sup>7-10</sup> The understanding of the nucleation process of this layer is a crucial problem for those fabricating HgCdTe-based, large-format, infrared focal plane arrays. Some studies have addressed this problem and postulated preliminary models of the initial stages of ZnTe growth.<sup>7-10</sup> In previous work, we have demonstrated experimentally the location of the As and Te on the Si(112) surface.<sup>11</sup> In that study, Te preferentially chemisorbed at step edges and As preferentially

(Received December 6, 2006; accepted January 23, 2007; published online July 6, 2007)

chemisorbed on the terraces. The substrate surface characteristics influence the overall MBE growth kinetics leading to the formation of a rich variety of surface morphologies. This variety of morphologies poses a challenge to our understanding of heteroepitaxial growth. A more detailed understanding the ZnTe nucleation process for our standard growth methodology should assist those working in high-quality large-area B-face CdTe for the subsequent growth of HgCdTe epilayers.

In the present work, we undertake a detailed study of the initial stages of the heteroepitaxial of HgCdTe/CdTe/ZnTe/As-Si(112) layer formation. We use ion scattering spectroscopy (ISS), x-ray photoelectron spectroscopy (XPS), and reflection-high energy electron diffraction (RHEED) to study the ZnTe layer formation on the As-Si(112) surface. Within this scenario, it is of primary importance to optimize the growth of ZnTe epitaxial layers by studying their microstructural and morphological properties.

## EXPERIMENTAL

The Si(112) surface was hydrogen passivated *ex situ* using a recipe proven to give excellent inert characteristics.<sup>12</sup> Upon loading the substrate into the MBE chamber, the H was desorbed by ramping to 700°C, while exposing the surface to an As<sub>4</sub> flux. During this process, the Si(112) surfaces are passivated with an As monolayer, producing a surface for subsequent deposition of ZnTe by MEE. The ZnTe layers were grown by alternating Zn and Te<sub>2</sub> fluxes with the substrate held at 290°C. The full process consists of 60 cycles; however, 3, 6, 9, 12, 15, 30, and 60 cycles were individually grown and then transferred *in vacuo* to the surface analysis system to monitor the initial stages of the ZnTe nucleation process. This procedure was closely monitored by observing the RHEED pattern. In addition, RHEED patterns of full CdTe/ZnTe/As-Si and ZnTe/As-Si (after annealing at about 450°C under Te overpressures) structures were recorded for comparison. Thick films of pure Zn and Te were used as standards. The XPS wide scans were obtained at a base pressure of  $5 \times 10^{-10}$  torr with either Mg K<sub>α</sub> at 1253.6 eV or monochromatized Al K<sub>α(1,2)</sub> x-rays with energy of 1486.6 eV. The XPS pass energy was set to 187.85 eV to ensure good signal to noise for the inelastic background analysis. The ISS measurements were performed at a Ne base pressure of  $2 \times 10^{-9}$  torr, using 2 keV <sup>20</sup>Ne<sup>+</sup> ions with a landing current of 10 nA. The ion gun and analyzer were positioned at a scattering angle of 134° to avoid most of the background signals originating from neutrals, reionized ions, and most secondary events.

## RESULTS AND DISCUSSION

### Te Termination of the ZnTe Layer (B Face)

The examination of the early stages of ZnTe formation is important to verify and understand the

current process as well as to optimize the growth parameters. In addition, by optimizing the ZnTe growth process, improvements to the ZnTe layer quality and thus an overall reduction of defect density in the CdTe and HgCdTe can be expected. The B-face CdTe and HgCdTe epilayers can be achieved when the Si surface is passivated with As and the ZnTe buffer layer is deposited by MEE.<sup>1,2</sup> Here, we attempt to provide experimental evidence that the ZnTe layer is Te terminated, thus making available a B-face template for the CdTe formation. Due to the high neutralization probabilities and scattering cross sections of low energy ions, ISS enables the selective analysis of the outermost atomic layer.<sup>13</sup> The elastic binary collisions of <sup>20</sup>Ne<sup>+</sup> ions provide an energy spectrum that is characteristic of the distribution of the masses of the surface atoms.

Figure 1 illustrates the ISS spectra after (a) three cycles, (b) six cycles, and (c) nine cycles during MEE growth of ZnTe. The spectrum after three cycles clearly shows prominent As and Te peaks at about 0.392 and 0.583, respectively; there is also a very small peak at 0.339 corresponding to Zn. However, after six and nine cycles, the Zn and Te peak intensities increase, while the decreasing As peak is indicative of the ZnTe covering the Si(112) surface. The exponential increase of the Te signal and decay of As peak indicate a uniform deposition and distribution of the ZnTe layer. It is important to notice that only after nine cycles had the As signal nearly vanished, indicating a low sticking coefficient for the first ZnTe layer. Figure 2 depicts the XPS spectra after nine cycles of Zn and Te exposure, at a take-off angle (TOA) of 75° (solid line) and 25° (dashed line). In addition, the XPS data in Fig. 2 show normal attenuation of the Si and As signals consistent with thin uniform layer attenuation, specifying a nearly full first layer formation after

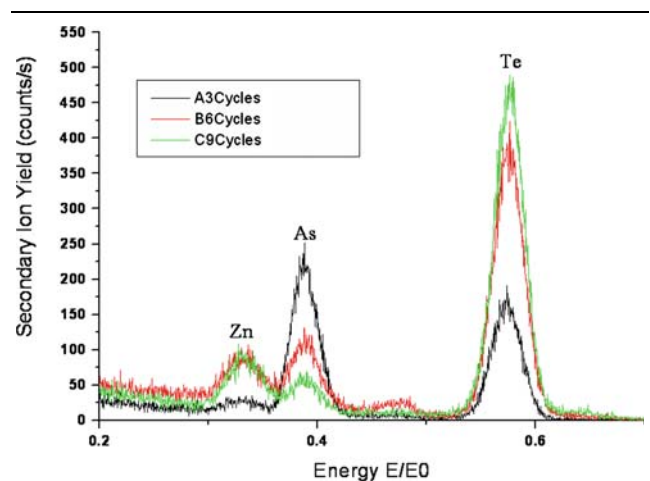


Fig. 1. ISS of the initial nucleation stages from a ZnTe buffer layer on the As-terminated Si(112) surface: (a) after three cycles, (b) after six cycles, and (c) after nine cycles of Zn and Te exposures of our standard process during the MEE growth of a ZnTe layer.

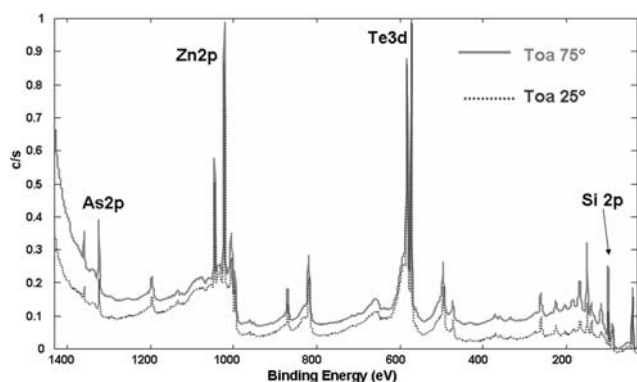


Fig. 2. XPS spectra after nine cycles of Zn and Te exposure, at a TOA of 75 (solid line) and 25 (dashed line). The data show attenuation of the Si and As signals, indicating a thin layer after nine cycles.

nine cycles. There is no evidence after nine MEE cycles of thick island formation, because the Si2p and As2p signals are normally attenuated due to the ZnTe overlayer, as shown in Fig. 2. We take the observation of these two substrate signals as evidence of very thin ZnTe layer formation.

The relative Te signal strength of the ISS data in Fig. 1 designates a Te-terminated surface. Further evidence is provided by comparison of the Zn2p/Te3d intensity ratio of the surface versus bulk signals. The surface sensitive XPS data (TOA 25°) in Fig. 2 demonstrate a reduction of the Zn2p/Te3d signal intensity compared to the bulk (TOA 75°) Zn2p/Te3d signal intensity, indicating Te is at the top of the surface layer. The ISS along with non-destructive depth profiles by angle-resolved XPS clarifies and supports that MEE of ZnTe/As-Si nucleates B face.

### IN-SITU RHEED CRYSTALLOGRAPHIC OBSERVATIONS

Due to its extreme surface sensitivity (top ~10 Å probed),<sup>14</sup> RHEED was used to assess the crystalline quality of ZnTe formation on Si(112). In RHEED, a streaky diffraction pattern is indicative of smooth slightly disordered two-dimensional film growth, while a typical transmission spot diffraction pattern results from undesirable surface faceting or three-dimensional (islandlike) growth. Figure 3 shows the RHEED patterns of the early stages of ZnTe growth for (a) after hydrogen passivating, (b) As exposure, (c) initial 25 s Te exposure, (d) three-cycle MEE, (e) six-cycle MEE, and (f) nine-cycle MEE ZnTe deposition. The RHEED patterns of the MEE grown ZnTe clearly contrast that of the H-terminated, As-passivated, and after 25 s Te-exposed Si (112) substrate. A  $1 \times 2$  reconstruction is observed for the H-terminated surface, while a  $2 \times 4$  reconstruction is obtained for the As-passivated and Te-exposed surfaces. For the nucleation of ZnTe after three cycles (d), the ZnTe RHEED

pattern becomes barely visible. After six cycles of MEE ZnTe deposition (Fig. 3e), the ZnTe pattern is more distinct and the Si streaks are no longer visible along the  $\langle 110 \rangle$  azimuth. The RHEED pattern obtained after nine cycles indicates high defect density layer-by-layer staircase-step growth.

Figure 4 shows the RHEED patterns of MEE grown ZnTe after (a) 30 and (b) 60 cycles. Figure 4c is the ZnTe RHEED pattern after 545°C anneal, and Fig. 4d shows the RHEED pattern after the end of a 10- $\mu\text{m}$  CdTe growth. The RHEED patterns observed for the 30- and 60-cycle MEE ZnTe growth display staircase step and faceting surface structure. After the ~450°C ZnTe anneal (Fig. 4c), the RHEED pattern becomes more defined and brighter, suggesting a more ordered crystallographic structure. At the end of the CdTe growth, reduced disorder in the  $\langle 110 \rangle$  direction (indicated by decreased streak width) as compared to the annealed ZnTe epilayer is observed by RHEED (Fig. 4d).

### DETERMINATION OF THE SURFACE MORPHOLOGY AND THE COVERAGE BY QUASES™

In order to better understand the details of the ZnTe nucleation process on the Si(112) substrate, the energy loss structure that accompanies XPS was used to study surface morphology. Information about the overlayer morphology and coverage can be derived from the Tougaard analysis algorithm (QUASES),<sup>15,16</sup> which takes into account the peak intensity, the peak shape, and the background of the measured energy spectra. QUASES theoretical framework has previously been described in detail.<sup>15–18</sup> The XPS spectra processing is facilitated by a commercial software package QUASES-Tougaard. This method enables us to distinguish between standard surface morphologies, e.g., uniform overlayer, islandlike growth, continuous concentration profiles, and a buried layer.

Here, Te photoelectrons are used to analyze the lateral and depth distribution of the ZnTe layer on the Si(112) surface. To calibrate the inelastic background, an MBE-deposited Te thick film is used as a reference spectrum. Figure 5 depicts quantitative model predictions from inelastic-background QUASES analysis of (a) three-cycle and (b) six-cycle ZnTe formation on Si(112). These figures show the best fit of the reference Te spectrum (solid line) to the experimental spectrum (dashed line) from (a) three cycles and (b) six cycles of MEE ZnTe. After three cycles of ZnTe deposition, the XPS Te signal is best fitted with a Te surface coverage of approximately 83% at 1.9 Å thickness. For the six-cycle ZnTe sample, the best fit is obtained with 85% Te surface coverage at 2.9 Å thickness, and the remaining 15% of the surface has a 4.2 Å thick Te layer. It should be noted that the total uncertainty in the parameters used in the fit has been shown experimentally to amount to less than 10%.<sup>19</sup>

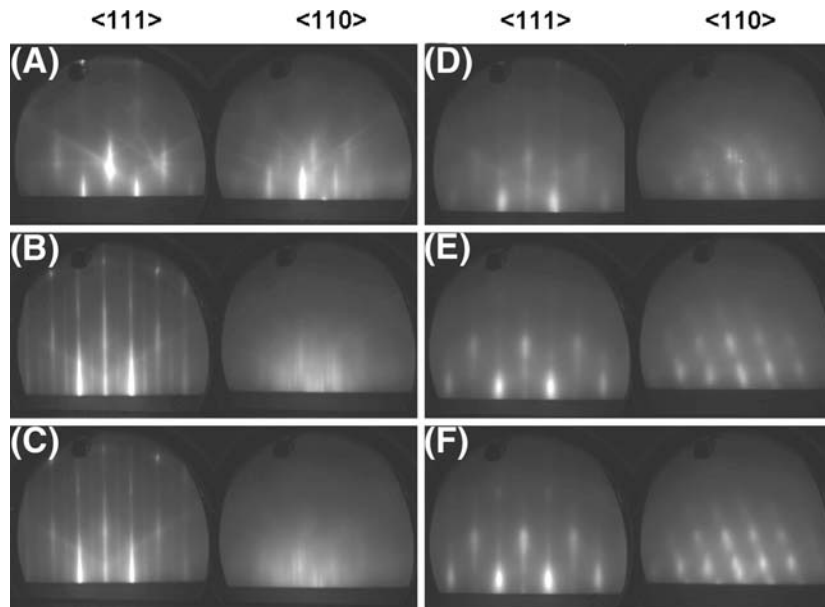


Fig. 3. RHEED patterns at every step of the ZnTe formation process on the Si(112) surface, where (a) is after hydrogen passivated, (b) after As exposure, (c) after an initial 25 s Te exposure, (d) three cycles MEE, (e) six cycles MEE, and (f) nine cycles MEE.

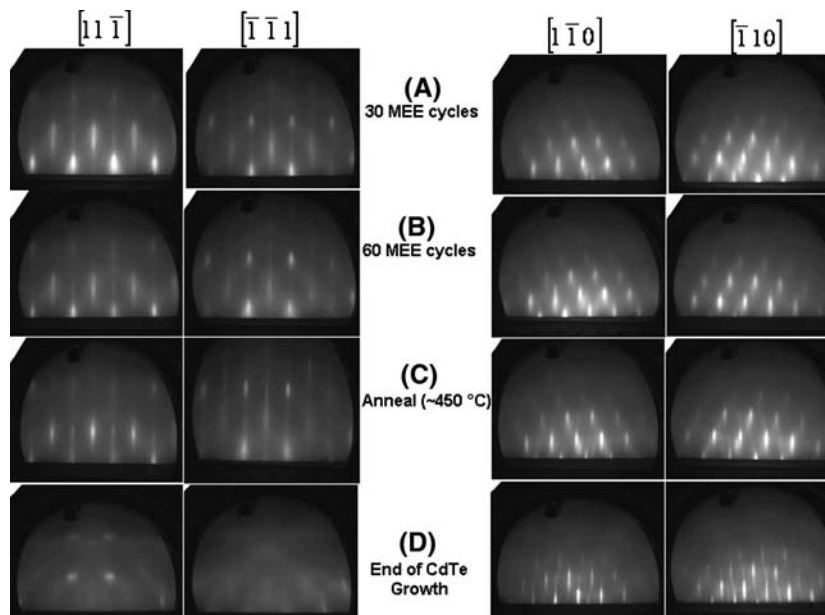


Fig. 4. RHEED of MEE grown ZnTe after (a) 30 cycles, (b) 60 cycles, and (c)  $-450^{\circ}\text{C}$  annealing. (d) Typical patterns after the end of the CdTe growth.

A similar approach for the nine-cycle MBE grown provides a surface coverage of 23% with a 2.9 Å layer, while a thicker layer of about 5.8 Å covers another 77% of the surface. At 15 cycles MEE growth, a surface coverage of 8% with a 8.3 Å layer and a thicker layer of about 12 Å covers another 92% of the surface. For the 15-cycle MEE ZnTe deposition, the results were complemented with a film thickness calculation using the normal atten-

uation in variable angle XPS. This analysis produced 10 Å average layer thickness. We take this as evidence that the inelastic-background calculation is accurate in providing the thickness of the ZnTe layer as well as providing confidence in our QUASES analysis. The 30-cycle ZnTe deposition results in a Te surface coverage of 8% with a 13 Å layer, and a thicker layer of about 17 Å covers the remaining 92% of the surface. Finally, the 60-cycle ZnTe deposition

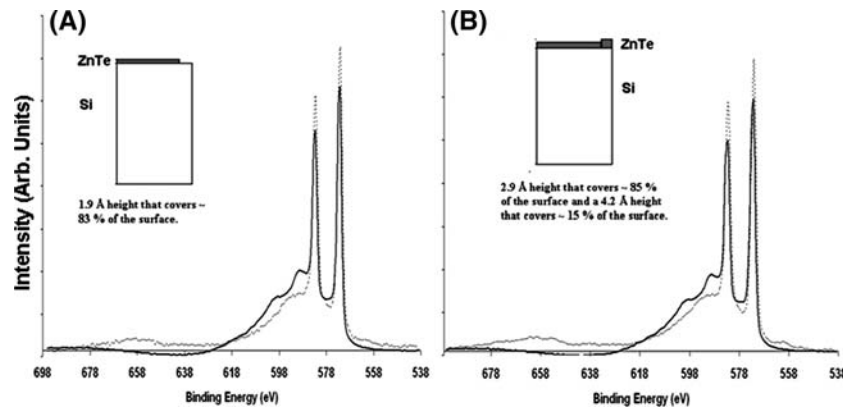


Fig. 5. Models of the ZnTe formation on Si(112) obtained using QUASES generated with a spectra from a thick pure Te MBE layer acting as a reference (solid line). The experimental spectrum (dashed line) is from (a) a three-cycle and (b) a six-cycle MEE ZnTe procedure.

produces 8% Te coverage with a 24 Å layer, and a thicker layer of about 26 Å covers the remaining 92% of the surface. The thickness of the full ZnTe deposition of 60 cycles is substantially thinner than the expected one monolayer per cycle formation. The results show that detailed information about the nucleation of ZnTe epitaxial formation can be obtained using the QUASES algorithm. Furthermore, the technique reveals lateral and depth distribution of the ZnTe layer, complementing and clarifying the results from the ISS and RHEED analysis.

## CONCLUSIONS

In summary, the results indicate a reduced rate MEE ZnTe epitaxial layer formation. However, the structure obtained is consistent with B-face ZnTe epilayer. RHEED and QUASES analysis shows the formation of a nearly complete layer at six MEE ZnTe cycles. Inelastic background analysis predicts full coverage with 2.9 Å and 4.2 Å thick layers, covering 85% and 15% of the surface, respectively. The faceting and thin islanding formation indicated by RHEED is fully consistent with the QUASES analysis. However, ISS indicates that nearly complete coverage requires nine cycles of ZnTe deposition. The initial stages of nucleation show no indication of thick island formation. Further efforts will be directed at optimizing the nucleation of ZnTe for a potential two-dimensional growth or layer-by-layer formation.

## REFERENCES

1. H. Shtrikman, M. Oron, A. Raizman, and G. Cinader, *J. Electron. Mater.* 17, 105 (1988).
2. R. Sporcken, S. Sivananthan, K.K. Mahavadi, G. Monfroy, M. Boukerche, and J.P. Faurie, *Appl. Phys. Lett* 55, 1989 (1989).
3. Y.P. Chen, S. Sivananthan, and J.P. Faurie, *Electron. Mater.* 22, 951 (1993).
4. Y.P. Chen, J.P. Faurie, S. Sivananthan, G.C. Hua, and N. Otsuka, *J. Electron. Mater.* 24, 475 (1995).
5. Y. Xin, N.D. Browning, S. Rujirawat, S. Sivananthan, Y.P. Chen, P.D. Nellist, and S.J. Pennycook, *J. Appl. Phys.* 84, 4292 (1998).
6. A. Million, N.K. Dhar, and J.H. Dinan, *J. Cryst. Growth* 159, 76 (1996).
7. N.K. Dhar, C.E.C. Wood, A. Gray, H.Y. Wei, L. Salamanca-Riba, and J.H. Dinan, *J. Vac. Sci. Technol. B* 14, 2366 (1996).
8. N.K. Dhar, P.R. Boyd, M. Martinka, J.H. Dinan, L.A. Almeida, and N. Goldsman, *J. Electron. Mater.* 29, 748 (2000).
9. N.K. Dhar, N. Goldsman, and C.E.C. Wood, *Phys. Rev. B* 61, 8256 (2000).
10. B. Brill, Y. Chen, N.K. Dhar, and R. Singh, *J. Electron. Mater.* 32, 717 (2003).
11. M. Jaime-Vasquez, M. Martinka, R.N. Jacobs, and M. Groenert, *J. Electron. Mater.* 35, 1455 (2006).
12. P.J. Taylor, W.A. Jesser, M. Martinka, K.M. Singley, J.H. Dinan, R.T. Lareau, M.C. Wood, and W.W. Clark III, *J. Vac. Sci. Technol. A* 17, 1153 (1999).
13. H.H. Brogersma and P.M. Mul, *Chem. Phys. Lett.* 14, 380 (1972).
14. J.E. Mahan, K.M. Geib, G.Y. Robinson, and R.G. Long, *J. Vac. Sci. Technol. A* 8, 3692 (1990).
15. S. Tougaard, *Surf. Interface Anal.* 11, 453 (1988).
16. S. Tougaard, *Surf. Sci.* 216, 343 (1989).
17. S. Tougaard, *J. Vac. Sci. Technol.* A8, 2197 (1990).
18. H.S. Hansen and S. Tougaard, *Surf. Interface Anal.* 17, 453 (1988).
19. M. Schleberger, A. Cohen Simonsen, and S. Tougaard, *J. Vac. Sci. Technol. A* 15, 3032 (1997).